ARCHIVES OF METALLURGY

Volume 47 2002 Issue 1

MARIAN KIELOCH*

MODEL STUDIES ON THE ENERGY-SAVING HEATING OF STEEL CHARGE

BADANIA MODELOWE ENERGOOSZCZĘDNEGO NAGRZEWANIA WSADU STALOWEGO

In order to perform the computer simulation of the effect of heating technology on heat consumption, a program for the numerical computations of charge heating and heat exchange in the furnace chamber was developed within this study.

The calculations of heat exchange in the furnace chamber were made using a zonal method.

The internal space of the furnace was divided into 20 computational zones, in which isothermal surfaces and isothermal gas bodies were separated.

The problem of radiation heat flow was solved using two versions of the brightness and configuration ratios method. In heat exchange calculations, heat transfer by means of convection was taken into account.

The results of the computer simulation of the effect of heating intensity on heat exchange indicate clearly that the most energy-saving process is heating with "nearly" linear variation of charge surface temperature.

The computation results show also that for each case of heating there is a specific charge surface temperature increase rate during the heating period, which assures the minimum heat consumption.

Dla przeprowadzenia symulacji komputerowej wpływu technologii nagrzewania na zużycie ciepła wykonano w pracy program obliczeń numerycznych nagrzewania wsadu i wymiany ciepła w komorze pieca. Obliczenia numeryczne nagrzewania wsadu wykonano posługując się metodą bilansów elementarnych.

Obliczenia wymiany ciepła w komorze pieca wykonano wykorzystując metodę strefową.

Wewnętrzną przestrzeń pieca podzielono na 20 stref obliczeniowych, w których wydzielono izotermiczne powierzchnie oraz izotermiczne bryły gazowe.

Zagadnienie radiacyjnego przepływu ciepła rozwiązano z wykorzystaniem dwóch wersji metody jasności i stosunków konfiguracji. W obliczeniach wymiany ciepła uwzględniono transport na drodze konwekcji.

* KATEDRA PIECÓW PRZEMYSŁOWYCH I OCHRONY ŚRODOWISKA, POLITECHNIKA CZĘSTOCHOWSKA, 42-200 CZĘSTOCHOWA, AL. ARMII KRAJOWEJ 19

Wyniki symulacji komputerowej wpływu intensywności nagrzewania na zużycie ciepła jednoznacznie wskazują, że procesem najbardziej energooszczędnym jest nagrzewanie z „prawie" liniową zmianą temperatury powierzchni wsadu.

Wyniki obliczeń wskazują również, że dla każdego przypadku nagrzewania istnieje ściśle określona szybkość wzrostu temperatury powierzchni wsadu w okresie podgrzewania, zabezpieczająca minimalne zużycie ciepła.

List of main denotations

a – temperature conductivity, m^2/s or m^2/h,
c – specific heat, $J/(kg \cdot K)$,
$\dot{E}_{bgi}$ – flux of radiation energy emitted by the gas body, W,
Fo – Fourier number,
$\dot{I}_1$ – flux of the total enthalpy of fuel, W,
$\dot{I}_d$, $\dot{I}_{od}$ – flux of the enthalpy of combustion gas carried away from a zone, W,
L – furnace length, m,
l – length of the heated charge, m,
l – ordinal number,
M – surface temperature increase rate, K/s or K/h,
N, P – constant quantities,
s – computational thickness of the heated plate, m,
t – temperature, $°C$,
w – furnace output, kg/h, t/h
W – heat capacity , J/K,
x – flat layer coordinate, m,
Δt – temperature difference, K,
V_i – volume of the i-th differential element, m^3,
ϱ – mass density, kg/m^3,
$\dot{Q}$ – heat flux, W,
q – unit heat consumption, kJ/kg,
λ – thermal conductivity, $W/(m \cdot K)$,
λ_i – thermal conductivity of the i-th element, $W/(m \cdot K)$,
τ – time, s or h.

charge; combustion gas; wall surface temperature; combustion gas temperature (version); furnace computational zone; furnace chamber

1. Introduction

Charge heating calculations are always associated with transient heat flow. Theoretical principles for these calculations are provided elsewhere, e.g. in works [1,2].

The process of heating a thick charge includes, as a minimum, the following two stages:

1. Heating up to a desired surface temperature, and
2. Soaking to obtain a desired temperature difference on the cross-section.

The first stage is normally assumed as heating in a medium of a known temperature (boundary conditions of type 3). This problem is broadly discussed in the literature. The

second stage is often accomplished under assumption of a constant surface temperature [3] (boundary conditions of type 2). Very often, for technological reasons, uniform heating occurs in the first stage, that is heating with maintaining the boundary conditions of type 1.

From among the known theoretical and experimental studies, derivations reported in work [4] are found the most useful in the analysis of energy-saving heating. In the present study, taking the thermodynamic analysis of soaking furnace operation as a starting point, it has been found that for any metal temperature such a fuel flux can be determined, for which the momentary thermal efficiency of the furnace chamber, $\overline{\eta}_t$, is maximum. Although this conclusion has been drawn upon assuming no temperature differences on the charge cross-section, nevertheless, as the results of theoretical derivations and model studies indicate, it can be generalized by the statement that only one technology exist for each particular heating process, which assures the maximum thermal efficiency of the process, and thus the minimum heat consumption.

2. Theoretical principles

The starting point for the consideration of transient heat flow is the Fourier-Kirchhoff differential equation:

$$\varrho \frac{\partial i}{\partial \tau} = \frac{\partial}{\partial x}\left(\lambda \frac{\partial T}{\partial x}\right) + \frac{\partial}{\partial y}\left(\lambda \frac{\partial T}{\partial y}\right) + \frac{\partial}{\partial z}\left(\lambda \frac{\partial T}{\partial z}\right) + \dot{q}_V. \tag{1}$$

For the purposes of developing a theoretical model of the heating process, the simplest technology was assumed for this process, which includes two stages (Fig. 1), namely:
Stage I – accomplished with a linear increase in charge temperature, and
Stage II – accomplished with a constant surface temperature.

At the same time, derivations were made by assuming the following simplifications:

- heating of a plate with infinite dimensions was assumed, where: $\frac{\partial}{\partial y}\left(\lambda \frac{\partial T}{\partial y}\right) = 0$, and $\frac{\partial}{\partial z}\left(\lambda \frac{\partial T}{\partial z}\right) = 0$,
- a heating process without forming scale and without phase transformations was assumed ($\dot{q}_V = 0$),
- a constant value of heat conductivity was assumed (λ = const), and $\partial i = c\partial t$, and
- variable thermal and physical properties of the charge and the heat of phase transformation were accounted for in the numerical computations.

For thus taken assumptions, Equation (1) can be written in the form as below:

$$\frac{\partial t}{\partial \tau} = a\frac{\partial^2 t}{\partial x^2}, \tag{2}$$

where:

$$a = \frac{\lambda}{c \cdot \varrho}. \tag{3}$$

The value of coefficient "a" is all-important, as it determines the temperature field on the cross-section of the heated plate.

As shown in work [5], the error made from assuming the constant value of a ($a = 5.625 \cdot 10^{-6}$ m^2/s) during the heating period is contained in the range $\pm 1.7\%$ for the heating rate in the interval from 72 to 720 K/h.

For the soaking period, the assumption of the constant value of a($a = 5.743 \cdot 10^{-6}$ m^2/s) results in a maximum error of $\pm 0.5\%$.

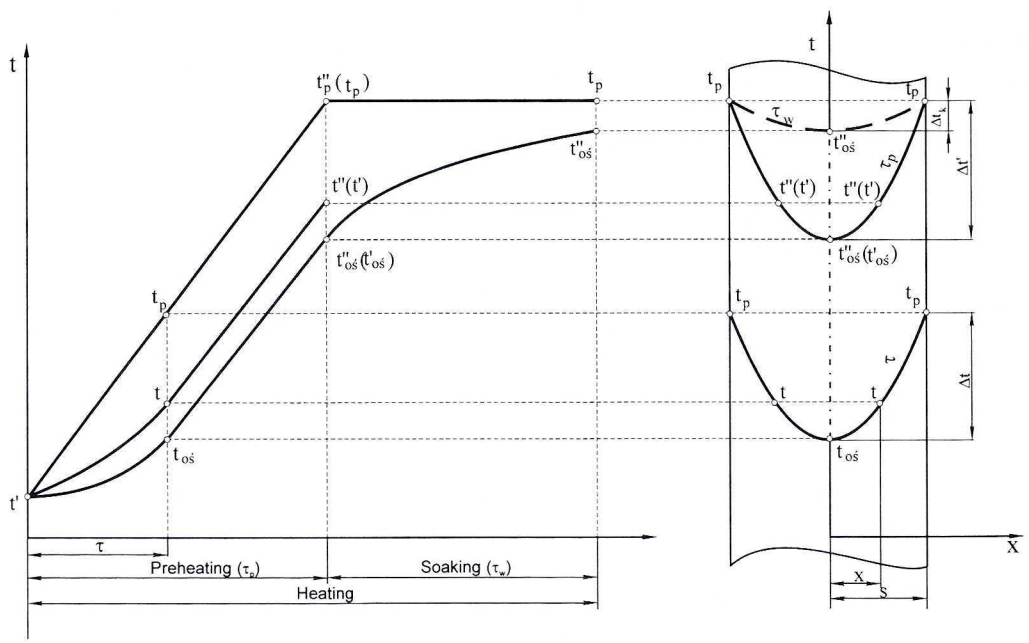

Fig. 1. Two-stage charge heating process

Based on derivations made in work [6], the relationship for the total time of a two-stage soaking process (Fig. 1) can be written in the following form:

$$\tau_n = \frac{t_p'' - t_p'}{M} + \frac{1}{P} \cdot \frac{s^2}{a_w} \cdot \ln\left\{ N \frac{Ms^2}{2a_p} \left[1 - N \exp\left(-P \frac{a_p}{s^2} \cdot \frac{t_p'' - t_p'}{M} \right) \right] \cdot \frac{1}{\Delta t_k} \right\}. \tag{4}$$

For long soaking times, if M is small, the value of $N \exp\left(-P \frac{a_p}{s^2} \cdot \frac{t_p'' - t_p'}{M} \right)$ is close to

zero, and then:

$$\tau_n = \frac{t_p'' - t_p'}{M} + \frac{1}{P} \cdot \frac{s^2}{a_w} \cdot \ln\left(N \frac{Ms^2}{2a_p} \cdot \frac{1}{\Delta t_k}\right). \tag{5}$$

Output for each type of furnace can be calculated from the formula below:

$$w = \frac{m}{\tau_n}. \tag{6}$$

For pusher furnaces, it will be:

$$m = 2s \cdot 1 \cdot L \cdot \varrho \cdot n. \tag{7}$$

Thus, the output of a pusher furnace can be described by the following relationship:

$$w = \frac{2P \cdot a_w \cdot s \cdot l \cdot L \cdot \varrho \cdot n \cdot M}{(t_p'' - t_p') \cdot P \cdot a_w + Ms^2 \cdot \ln\left\{N \frac{Ms^2}{2a_p}\left[1 - N \exp\left(-P \frac{a_p}{s^2} \cdot \frac{t_p'' - t_p'}{M}\right)\right] \cdot \frac{1}{\Delta t_k}\right\}}. \tag{8}$$

Whereas, for slow heating we have:

$$w = \frac{2P \cdot a_w \cdot s \cdot l \cdot L \cdot \varrho \cdot n \cdot M}{(t_p'' - t_p') \cdot P \cdot a_w + Ms^2 \cdot \ln N \cdot \frac{Ms^2}{2a_p} \cdot \frac{1}{\Delta t_k}}. \tag{9}$$

Using relationship (8), the effect of heating rate on the output of heating furnaces is described by the equation below:

$$w = \frac{aM}{b + c + M \cdot \ln\left\{d \cdot M\left[1 - e \cdot \exp\left(-\frac{f}{M}\right)\right]\right\}}. \tag{10}$$

If relationship (9) is used for the calculation of the output, then:

$$w = \frac{a}{b + c \cdot M \cdot \ln(d \cdot M)}. \tag{11}$$

Based on the results of performed computations it can be stated that an increase in heating intensity, as measured by surface temperature increase rate, causes a significant increase in the output of furnaces. With increasing heating rate incremental outputs decrease, and after exceeding a certain (rational) value of heating rate, its further increasing becomes irrational for thermal reasons, and in extreme cases it is no longer possible.

The main index for the evaluation of furnace operation [7] is heat per unit mass of heated charge, expressed in kJ/kg.

Theoretically, for heating without limitations in the rate of charge temperature increase, heat flux in furnaces will be composed of three main balance groups, as below:

- group 1 – for which heat flux $\dot{Q}_1$ is a linear function of furnace output, e.g. usable charge heat,
- group 2 – for which heat flux $\dot{Q}_2$ is independent of furnace output, e.g. cooling water heat, and
- group 3 – for which heat flux $\dot{Q}_3$ is dependent on furnace output, and thus on heating rate, M.

The value of heat flux $\dot{Q}_3$ can be determined from the relationship:

$$\dot{Q}_3 = \sum_{i=1}^{\infty} f_i(M^{n_i}). \tag{12}$$

In Equation (12), n_i is a constant dependent on heating rate, M, and different for each balance item.
Thus:

$$\dot{Q} = q_1 \cdot w + \sum_{i=1}^{\infty} \dot{Q}_{2i} + \sum_{i=1}^{\infty} f_i(M^{n_i}), \tag{13}$$

or:

$$q = q_1 + \frac{\sum_{i=1}^{\infty} \dot{Q}_{2i} + \sum_{i=1}^{\infty} f_i(M^{n_i})}{w}. \tag{14}$$

If the output of a furnace is described by relationship (8), then:

$$q = q_1 + \frac{\left[\sum_{i=1}^{\infty} \dot{Q}_{2i} + \sum_{i=1}^{\infty} f_i(M^{n_i})\right] \cdot \left\{(t_p'' - t_p') \cdot P \cdot a_w + Ms^2 \cdot \ln\left\{N\frac{Ms^2}{2a_p}\left[1 - N\exp\left(-P\frac{a_p}{s^2} \cdot \frac{t_p'' - t_p'}{M}\right)\right] \cdot \frac{1}{\Delta t_k}\right\}\right\}}{2P \cdot a_w \cdot s \cdot l \cdot L \cdot \varrho \cdot n \cdot M}, \tag{15}$$

or for slow heating:

$$q = q_1 + \frac{\left[\sum_{i=1}^{\infty} \dot{Q}_{2i} + \sum_{i=1}^{\infty} f_i(M^{n_i})\right] \cdot \left[(t_p'' - t_p') \cdot P \cdot a_w + Ms^2 \cdot \ln\left(N\frac{Ms^2}{2a_p} \cdot \frac{1}{\Delta t_k}\right)\right]}{2P \cdot a_w \cdot s \cdot l \cdot L \cdot \varrho \cdot n \cdot M}. \tag{16}$$

If only balance group 1 is taken into account in the considerations, then the value of heat consumption index will be independent of the rate of surface temperature increase, as well as of the output (Fig. 2). This is a purely theoretical case for heating furnaces.

For balance group 2, unit heat consumption will decrease, whereas for balance group 3 it will grow with increasing heating rate.

Considering the three balance groups, the relationship of unit heat consumption as a function of heating rate will have a minimum defined by the value of rational heating rate, $M_{\text{rac.}}$.

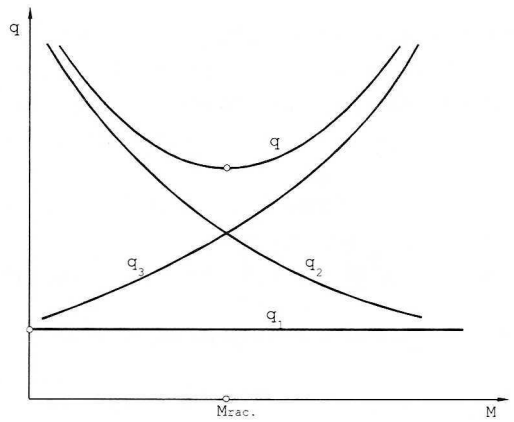

Fig. 2. Effect of heating rate on heat consumption index

For furnaces attaining low heat consumption indices, the value of heat stream $\dot{Q}_3$ is small, and it can be assumed that $\dot{Q}_3 = 0$, and then the following can be determined from relationship (14):

$$q = a + \frac{b}{w}. \tag{17}$$

3. Numerical modeling of heating up the charge

To determine accurately the physical heat of combustion gases leaving the furnace and cooling water heat in the heat balance, the calculation of heat exchange in the furnace chamber is necessary. The analytical calculation of these balance items are little accurate, therefore both the values of these items and charge heating were determined by means of numerical computations.

The numerical computations of charge heating were performed using the elementary balances method. This method allows the effect of temperature on the change of charge thermo-physical parameters and the occurrence of external heat sources (the heat of occurring phase transformations) to be taken into account [8].

The computations were made for the following assumptions:
- charge geometry – plate with infinite dimensions,
- heat flow direction – normal to the plate surface (the one-dimensional problem),
- charge thermo-physical parameters (λ and c_p) are dependent on temperature,
- a phase transition occurs in the charge,
- the temperature interval in which the phase transition occurs and the heat of phase transition are known,
- no phenomena associated with change in the conditions of heat exchange with the environment, or with heat release or absorption occurring on the charge surface,

- the initial temperature distribution on the charge cross-section is known, and
- condition for ending the computations – reaching the preset charge surface temperature and the preset final temperature difference on the charge cross-section.

In conformance with the principle of the elementary balances method, it was assumed that:

- nodes representing individual differential elements are located at their centres of gravity (geometrical centres),
- the heat capacities and outputs of external sources are concentrated at the nodes of differential elements,
- nodes representing charge surfaces are capacity-free,
- heat flow resistance is concentrated in the segments between the nodes.

For computations, division into elements of a constant volume of V_i = idem was made.

The basis for the computation of the temperature of any internal node, i, in the successive time interval is the energy balance equation:

$$\dot{Q}_{i-1,i} + \dot{Q}_{i+1,i} + V_i \cdot \dot{q}_{Vi} = W_i \frac{\Delta T_i}{\Delta \tau}. \tag{18}$$

The fluxes of heat flowing between the adjacent nodes i and j are determined by the relationship:

$$\dot{Q}_{ji} = K_{ji}(T_j - T_i). \tag{19}$$

Assuming that heat fluxes $\dot{Q}_{ji}$ are proportional to temperature differences at the moment corresponding to the k-th time step, node temperatures after the next time interval $(k+1)$ were determined based on Equation (18):

$$T_i^{k+1} = T_i^k + \frac{\Delta \tau}{W_i^k}[K_{i-1,i}(T_{i-1}^k - T_i^k) + K_{i+1,i}(T_{i+1}^k - T_i^k) + V_i \dot{q}_{V_i}^k]. \tag{20}$$

The above given formula represents the so called "explicit" differential scheme [9, 10]. The values of thermal conductivity λ and of unit heat capacity c are dependent on temperature. The relationships $\lambda = f(T)$ and $c = f(T)$ represented in a tabular form were used in computations. The values of λ and c for intermediate temperatures, contained between the temperatures specified in the tables, were determined by the linear interpolation method.

The occurrence of internal heat sources (the source member $V_i \cdot \dot{q}_{V_i}^k$) was taken into account only in the temperature range of a phase transition.

The condition for the physical accuracy of solutions determined by relationship (20) is a positive value of the coefficients occurring at the temperatures [9]. From this condition, the limitation of the time interval (step) $\Delta\tau$ results:

$$\Delta \tau \leq \frac{W_i}{K_{i-1,i} + K_{i+1,i}}. \tag{21}$$

Due to the above limitation, an attempt was also made to perform the computation of heating using the implicit scheme (the backward differential quotient method). According to this method, the values of temperature occur at the end of the considered time interval in the expressions defining the fluxes of heat flowing between the neighbouring nodes. Therefore, the energy balance equation takes on the following form:

$$K_{i-1,i}T_{i-1}^{k+1}-\left(K_{i-1,i}+K_{i+1,i}+\frac{W_i}{\Delta\tau}\right)T_i^{k+1}+K_{i+1,i}T_{i+1}^{k+1}=-\frac{W_i}{\Delta\tau}T_i^k-V_i\dot{q}_{V_i}^{k+1}. \quad (22)$$

Energy balance equations for all nodes of the region form a system in which the unknowns are the values of temperature in the nodes after the successive time interval $(k+1)$.

Solving of the system yields accurate results regardless of the length of the assumed time interval $\Delta\tau$.

The lack of limitations in the selection of $\Delta\tau$ represents a major advantage of the backward differential quotient method. On the other hand, the necessity of solving a system of equation for each time interval can be regarded as a drawback of this method.

A comparison of the results of computations of two-stage charge heating performed using, respectively, the explicit and implicit scheme was made in this study. Two-stage heating is characterized by a constant rate of surface temperature increase of $M=\frac{800}{3600}$ K/s at the first stage, and a constant surface temperature of T_p = 1523 K at the second stage.

The computations were made for a low-carbon steel charge of a thickness of 2s = 0.3m. The division of charge cross-section into 20 homogeneous differential elements and the following lengths of time interval were assumed:

- for the explicit scheme – $\Delta\tau$ = 1s,
- for the implicit scheme – $\Delta\tau$ = 1s, 2s and 5s.

The calculation results provide a basis for making the following observations:

- node temperature differences determined in the entire heating range by using the explicit and implicit schemes for any time τ and any node do not exceed 0.2 K (Tables 1, 2),
- the length of the assumed time interval has very little effect on the results of computations performed by the backward differential quotient method (Tables 1, 2).

Small differences in the results obtained using the above mentioned schemes are proof of their good accuracy.

During heating steel in the temperature range 727 to 912°C, the phase (allotropic) transformation $Fe_\alpha \rightarrow Fe_\gamma$ occurs.

The rate of this transformation depends on heating rate. There is no accurate information in the available literature, which would enable a detailed relationship to be established between the course of transformation and the rate of heating. By necessity, this problem has to be solved in an approximate way.

TABLE 1

Results of charge heating computations using the forward "p" ($\Delta\tau = 1$s) and backward "w" ($\Delta\tau = 1$s) differential quotients

No.	Heating time τ, s	Surface temp. t, °C	Axis temperature			Heat flux		
			t_p °C	t_w °C	$\lvert\Delta t\rvert$ K	$\dot{Q}_p$ W	$\dot{Q}_w$ W	$\lvert\Delta\dot{Q}\rvert$ %
1	1000	237.2	101.4	101.4	0.0	101944	104895	2.9
2	2000	459.4	269.8	269.7	0.1	122733	125260	2.0
3	3000	681.7	436.6	436.5	0.1	139424	141447	1.5
4	4000	903.9	586.7	586.6	0.1	147064	148682	1.1
5	5000	1126.1	724.8	724.7	0.1	160001	161669	1.0
6	6000	1250.0	903.7	903.6	0.1	106493	106586	0.1
7	7000	1250.0	1053.0	1052.9	0.1	60102	60154	0.1
8	8000	1250.0	1139.1	1139.0	0.1	34445	34486	0.1
9	9000	1250.0	1187.7	1187.6	0.1	19605	19635	0.2

TABLE 2

Results of charge heating computations using the forward "p" ($\Delta\tau = 1$s) and backward "w" ($\Delta\tau = 5$s) differential quotients

No.	Heating time τ, s	Surface temp. t, °C	Axis temperature			Heat flux		
			t_p °C	t_w °C	$\lvert\Delta t\rvert$ K	$\dot{Q}_p$ W	$\dot{Q}_w$ W	$\lvert\Delta\dot{Q}\rvert$ %
1	1000	237.2	101.4	101.6	0.2	101944	104802	0.1
2	2000	459.4	269.8	269.9	0.2	122733	125212	0.0
3	3000	681.7	436.6	436.6	0.1	139424	141382	0.0
4	4000	903.9	586.7	586.8	0.2	147064	148688	0.0
5	5000	1126.1	724.8	724.9	0.2	160001	161593	0.0
6	6000	1250.0	903.7	903.6	0.0	106493	106622	0.0
7	7000	1250.0	1053.0	1052.8	0.1	60102	60184	0.0
8	8000	1250.0	1139.1	1138.9	0.1	34445	34525	0.1
9	9000	1250.0	1187.7	1187.4	0.2	19605	19671	0.2

Very convenient for mathematical formulation is the assumption that the rate of transformation in a given differential element, in the assumed temperature range, corresponds accurately to the rate of change of the temperature of that element.

Under this assumption, the heat of transformation can be considered in the expression defining the heat capacity of the element:

$$W_i = (c + c_{prz}) \cdot \varrho \cdot V_i, \tag{23}$$

where:

$$c_{prz} = \frac{q_{prz}}{t_{p1} - t_{p2}}. \tag{24}$$

This formulation of the heat of transformation allows the source member ($\dot{q}_{V_i} = 0$) to be omitted in the energy balance equation. The value of the heat of transformation is $q_{prz} = 28.339$ J/kg [11].

A totally different approach to this problem was also made. A constant temperature of phase transformation was assumed. A nonzero source member $V_i \cdot \dot{q}_{V_i}$ occurs then in energy balance equations. A major shortcoming of this method of dealing with the problem is the necessity of controlling the progress of phase transformation in each differential element.

A comparison of the results of charge heating computations made using the above given methods of formulating phase transformation indicates only slight differences in the determined temperature distribution and the computed heating time. Therefore, the first formulation, as being easier for execution, was employed in computations made in this study.

A flow chart of charge heating computation is shown in Figure 3.

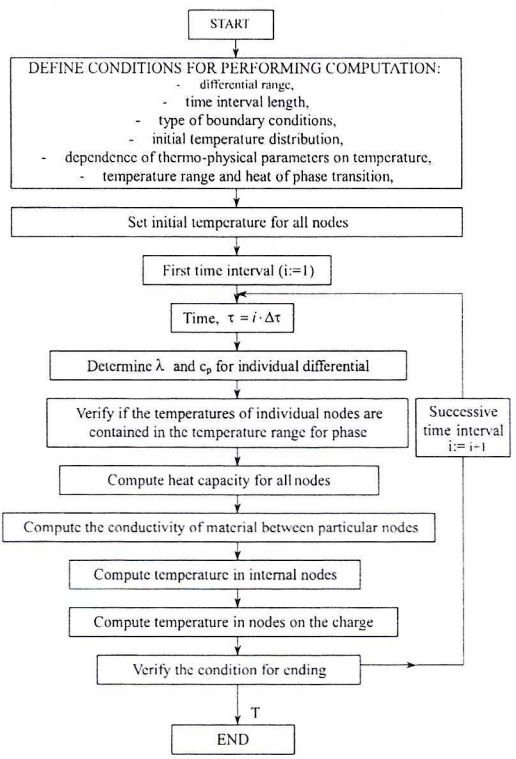

Fig. 3. Algorithm for charge heating computations

4. Numerical modeling of the temperature field in the furnace chamber

The execution of a selected technology requires maintaining a specific temperature field in the furnace chamber. This field is determined by the adopted technology, the type of charge (geometry, material, the initial temperature state) and the characteristics of furnace construction.

A mathematical model of heat exchange in the furnace chamber forms a basis for the computational determination of the required temperature distribution.

This paper presents a method of determining temperature field distribution in a pusher furnace. It was assumed that heating operations would be conducted in a fuel heating furnace, whose schematic diagram is shown in Fig. 4.

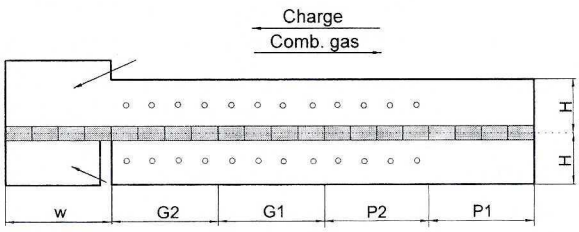

Fig. 4. Technological diagram of a heating furnace

The furnace space was divided conventionally into 5 technological zones and 20 computational zones by using planes perpendicular to the longitudinal axis of the furnace. The gas body, the furnace wall surfaces and the charge surfaces in each of the zones are regarded as being isothermal.

It is assumed that the heat of combustion gas is transferred to the charge surface and the furnace masonry surface by means of radiation and convection. Also, radiation heat exchange occurs between the masonry surface and the charge surface, as well as between separated furnace zones.

To solve the problem of radiation heat exchange, the brightness and configuration ratios method was employed in two versions. The versions of the method differ in the way by which heat flow between zones is determined. A comparison of computation results obtained by using particular versions of the method was made.

The coefficients of convection heat exchange (convective heat-transfer coefficients) were determined based on relationships applicable to flow in channels. As characteristic parameters, the average velocity of combustion-gas flow in a given zone and the substitute (hydraulic) diameter of the flow cross-section were assumed.

A preselected charge heating technology is determined by the distribution of densities of heat flux taken up by the surface of the charge over its length and the distribution of charge surface temperature. To determine these two distributions, the computations of charge heating are required to be carried out.

The mathematical model of heat exchange in a furnace is made of:

- relationships representing convective heat-transfer coefficient as a function of combustion-gas velocity,
- equations defining the fluxes of energy flowing between the surfaces and zones,
- expressions defining surface brightness, and
- energy balance equations.

The provided relationships enable one to build a system of nonlinear equations, the solution of which will be the values of temperatures determined.

The considered radiation-convection heat exchange system covers:

- surfaces of internal furnace walls,
- charge surfaces,
- imaginary vertical surfaces dividing the furnace chamber into zones,
- an imaginary horizontal surface situated in the mid-thickness of the charge, dividing the furnace chamber into the lower and upper parts, and
- combustion gas filling the furnace chamber.

It is assumed that:

- furnace wall and charge surfaces are all grey,
- the imaginary vertical surfaces are permeable to combustion gas, and
- the imaginary horizontal surfaces ideally reflect radiation and are not permeable to combustion gas.

Following the principle of the brightness and configurations ratio method it is assumed that the surfaces (planes) or the conventional division of the furnace emit and absorb radiation. The irradiation of one zone of the apparent surface is equal to the brightness of the other side of this surface.

The properties of apparent surfaces are the same as those of bodies subject to L a m b e r t ' s law. The radiation properties of a gas body and a surface in each of the created furnace zones are regarded as known. It is assumed that the brightness of the surfaces of the furnace walls and roof is the same.

The brightness of surface elements is calculated as the sum of internal emission and reflected radiation. Thus, the brightness of the charge surface (flat surface) will be:

$$F_1\dot{h}_1 = F_1\dot{e}_1 + (1-\varepsilon_1)\cdot(F_2\dot{h}_2\varphi_{2-1}\tau_{2-1} + F_{pp}\dot{h}_{pp}\varphi_{pp-1}\tau_{pp-1} + F_{p1}\dot{h}_{p1}\varphi_{p1-1}\tau_{p1-1} + F_1\dot{e}_g). \tag{25}$$

Similarly, the brightness of the wall and roof is defined:

$$F_2\dot{h}_2 = F_2\dot{e}_2 + (1-\varepsilon_2)\cdot\begin{pmatrix} F_1\dot{h}_1\varphi_{1-2}\tau_{1-2} + F_2\dot{h}_2\varphi_{2-2}\tau_{2-2} + F_{pp}\dot{h}_{pp}\varphi_{pp-2}\tau_{pp-2} + \\ + F_{p1}\dot{h}_{p1}\varphi_{p1-1}\tau_{p1-2} + F_2\dot{e}_g \end{pmatrix}. \tag{26}$$

The brightness of apparent surfaces is:

$$F_{pi}\dot{h}_{pi} = F_{1j}\dot{h}_{1j}\varphi_{1-pi}\tau_{1-pi} + F_{2j}\dot{h}_{2j}\varphi_{2-pi}\tau_{2-pi} + F_{pj}\varphi_{pj-pi}\tau_{pj-pi} + F_{pi}\dot{e}_{gj}. \tag{27}$$

The index "i" denotes the apparent surface of a given surface, situated on the left (l) or right (p) side. The index "j" relates to the elements of the neighbouring zone, adjacent to that apparent surface i.

For a preselected heating technology (heating process), charge surface temperature is a definite quantity in each zone. Heating computations enable also the determination of the density of heat flux $\dot{q}_1$ transferring into the charge surface. The following remain unknown quantities:

- wall surface temperature,
- gas body temperature, and
- combustion-gas flow rate.

Wall surface temperature and gas body temperature in each zone are determined from the energy balance equation for the charge surface and wall surface. Assuming that the control shields are situated immediately at the surface, the energy balance equations have the following form:

- for charge surface:

$$F_1\dot{q}_1 = F_1\dot{e}_g + F_2\dot{h}_2\varphi_{2-1}\tau_{2-1} + F_1\alpha_1(T_g - T_1) + F_{p1}\dot{h}_{p1}\varphi_{p1-1}\tau_{p1-1} + F_{pp}\dot{h}_{pp}\varphi_{pp-1}\tau_{pp-1}, \tag{28}$$

- for wall surface:

$$F_2\dot{q}_2 = F_2\dot{e}_g + F_1\dot{h}_1\varphi_{1-2}\tau_{1-2} + F_1\alpha_1(T_g - T_1) + \\ + F_{p1}\dot{h}_{p1}\varphi_{p1-2}\tau_{p1-2} + F_{pp}\dot{h}_{pp}\varphi_{pp-2}\tau_{pp-2}. \tag{29}$$

The density of heat flux $\dot{q}_2$ transferring through the wall is proportional to overall heat transfer coefficient k and the difference between internal wall surface temperature T_2 and ambient temperature T_{ot}:

$$\dot{q}_2 = k(T_2 - T_{ot}). \tag{30}$$

The energy balance equation for the gas body has the form of:

$$\dot{I}_d + \dot{I}_i + F_1\dot{h}_1A_{1-g} + F_2\dot{h}_2A_{2-g} + F_{p1}\dot{h}_{p1}A_{p1-g} + F_{pp}\dot{h}_{pp}A_{pp-1} = \dot{I}_{od} + F_1\varepsilon_1\dot{e}_g + \\ + F_2\varepsilon_2\dot{e}_g + F_{p1}\dot{e}_g + F_{pp}\dot{e}_g + F_1\alpha_1(T_g - T_1) + F_2\alpha_2(T_g - T_2) + \dot{Q}_s \tag{31}$$

The gas body energy balance is a basis for the determination of the flux $\dot{V}_g$ of fuel supplied to the zone and then to the determination of the flux of combustion-gas delivered to, and carried away from particular zones.

The brightness and configuration ratios method contains a simplification of assuming that the apparent surfaces (resulting from the division of the furnace into zones) radiate following Lambert's law. In reality, radiation energy fluxes passing through the apparent surface have a directional nature, being strictly dependent on the geometry of the entire system. The method of direct exchange surface and total exchange surface [12] is free from this simplification. This method has, however, the drawback of greatly increasing numerical task size with increasing number of zones. Obtaining the final result requires multiple solving of extensive systems of equations.

A modified version of the brightness and configuration ratios method applied in the present study substantially mitigates the problem of equation dimensions and, at the same time, reduces to a minimum the effects of the simplification that characterizes the method in its basic version.

The key to the modification is separating out a region around each zone, which covers several closest situated zones. The zone to which a particular region is designated occupies the central position in that region. This principle is not applicable to zones at the beginning and at the end of the furnace. It is assumed that apparent surfaces separating the isothermal elements of a region do not participate in radiative heat exchange. The only exception are the apparent surfaces constituting the boundary of the region. These surfaces are assumed to emit radiation following the principle adopted in the basic version of the method.

Therefore, the influence of the isothermal surface and volume elements of all zones situated in the described region are considered in the computations of radiation heat exchange. The influence of the elements of farther zones (beyond the region) is covered by the brightness of apparent surfaces at the region boundary.

The brightness of the surface elements of each zone is defined by the relationship:

$$\bigwedge_{i=1\ldots n} F_i \dot{h}_i = F_i \dot{e}_i + (1-\varepsilon_i)\left(\sum_1^k F_k \dot{h}_k \varphi_{k-i} \tau_{k-i} + F_i \sum_1^m e_{g_{m-i}} \tau_{m-i}\right). \tag{32}$$

Transmissibility for radiation passing through l isothermal gas bodies is determined from the relationship:

$$\tau_{i-j} = \exp\left(-\sum_{s=1}^{s=1} K_s \cdot r_s\right). \tag{33}$$

Absorption coefficient K_s is a function of gas body temperature and emission source temperature. It is calculated from the formula:

$$K_s(T_g, T_w) = \frac{1}{L} \ln \frac{1}{1-A_g}. \tag{34}$$

The system of energy balance equations provides the final basis for determining unknown temperatures. The general form of energy balance equation for a surface element is as follows:

$$\dot{E}_{r,i} + \dot{Q}_{ai} = \dot{E} + \dot{Q}_i. \tag{35}$$

Energy balance for a volume element has the form of:

$$\dot{I}_1 + \dot{E}_{r,i} + \dot{I}_{di} = \dot{I}_{wi} + \dot{Q}_{ai} + \dot{E}_{bgi} + \dot{Q}_s. \tag{36}$$

Similarly as in the case of the brightness and configuration ratios method, the equations of energy balance of surface elements are used for the computation of wall surface and gas body temperatures in the zone. The energy equation for the volume element serves for determining the amount of fuel supplied to the zone.

At the first stage, computations are performed by using the brightness and configuration ratios method in its basic version. After obtaining convergent solutions, computations by the modified method are continued. These computations include, in succession:

– determining the properties of radiative gas bodies,
– computing the brightness of surfaces from the system of equations (32), and
– solving the system of energy equations.

The computations are repeated until convergent solutions are obtained.

The presented methods were employed for modeling the temperature field in a pusher furnace, in which a predefined charge heating technology is executed.

Owing to the symmetry of phenomena, only heat exchange in zones above the charge axis is considered. For the modified version of the method it was assumed that regions designated to individual zones cover the three closest situated zones on each side. The results of modeling (Fig.5) obtained by the described methods are similar. Significant differences in the values of determined temperatures occur only in the first zone.

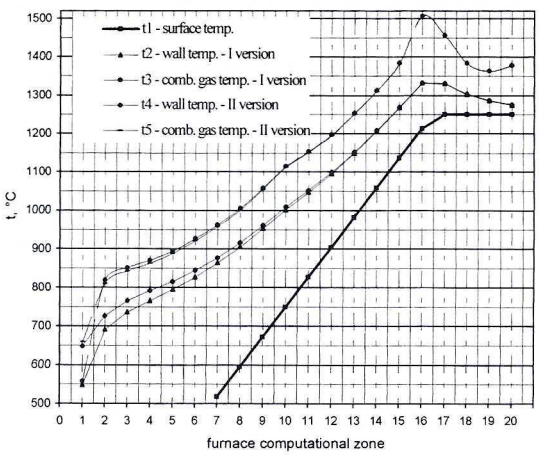

Fig. 5. Results of modeling for M = 400 K/h and G = 1.0

The results of modeling shown in Fig. 5 apply to the theoretical case where surface temperature increase changes according to a linear relationship.

If the surface temperature varies in a manner similar to that for real heating processes and is described by the relationship:

$$t_p = t_0 + M \cdot \tau^G, \tag{37}$$

then the differences in modeling results are smaller.

Because of the higher temperature of combustion gas leaving the furnace, unit heat consumption computed using the second method is a little higher and the thermal efficiency of the furnace is slightly smaller.

For example, when heating a 0.3 m thick steel charge at a surface temperature increase rate of M = 400 K/h, we obtain $\Delta \dot{q} = -6.1\%$.

If surface temperature increase rate is described by equation (37), then for G = 0.6-0.8, ten we have $|\Delta q| < 1\%$.

These differences only occur in the first computational zone and do not have any practical importance, because heat consumption in these zones, has a negative value for the both computational methods, anyway.

The algorithm for the computation of heat exchange in the furnace chamber is shown in Fig. 6.

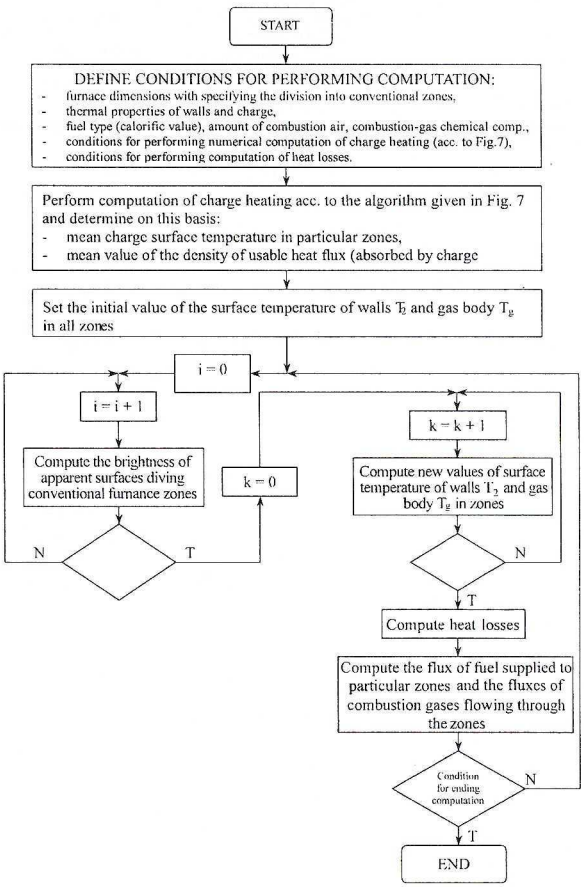

Fig. 6. Algorithm for the computation of heat exchange in the furnace chamber

5. Computer simulation of the effect of heating rate on heat consumption

Accomplishing heating at a specified rate of surface temperature increase and with soaking the charge to a preset temperature difference on the cross-section requires maintaining a specified temperature field within the furnace chamber. This temperature field is determined by the type of charge (as defined by its geometry, chemical composition, and the initial temperature distribution), the characteristics of furnace construction and, in each case, the assumed heating rate. For each heating rate, a furnace

chamber temperature field was separately established, which assured maintaining preset heating parameters, namely:

– final value of surface temperature, t_p = 1250°C, and
– final temperature difference on the charge cross-section, Δt_k = 50 K.

The computations of the effect of heating rate on unit heat consumption were carried out for three cases of furnace operation, namely:

1. for an ideal process,
2. for a furnace attaining high heat consumption indices, and
3. for a furnace attaining low heat consumption indices.

As the ideal process, such a process was understood, whose balance on the input side (Fig.7) was only composed of the chemical heat of fuel, whereas of the usable heat of the charge on the output side.

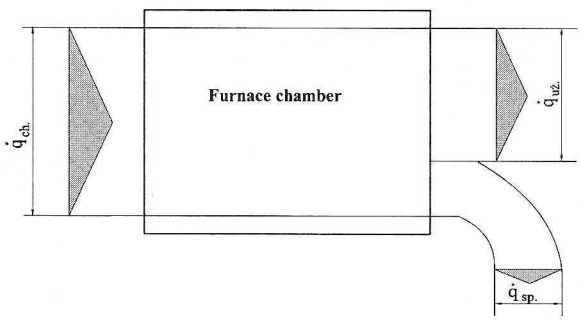

Fig. 7. Sankey's heat balance diagram for the ideal process

To secure the assumed variation of charge surface temperature, it is necessary to supply appropriate heat fluxes to the separated computational zones of the furnace. An example distribution of heat flux values for M = 500 K/h is shown in Fig.8.

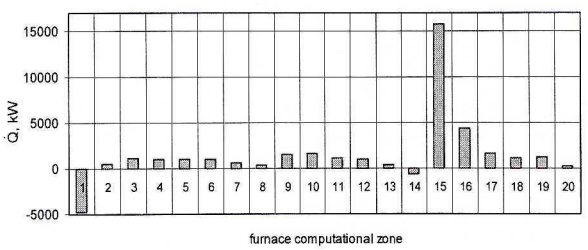

Fig. 8. Heat consumption in particular computational zones for M = 500K/h

It is evident that in order to achieve the specified surface temperature increase, zones exist, from which the heat should be withdrawn (the negative value of heat flux). The number of those zones, their distribution over the furnace length, as well as their associated heat flux values, all depend on heating rate, M.

Figure 9 illustrates the effect of the values of M on the sum of negative values of heat fluxes.

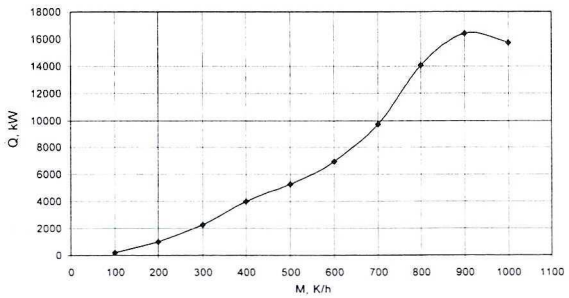

Fig. 9. Effect of heating rate on the sum of negative heat flux values

The higher rates of surface temperature increase, the larger the sums of negative heat flux values are.

There are two ways of heating process possible:

1. Maintaining the accurately linear increase of charge surface temperature. For this heating, heat should be carried away from some computational zones. This heat will be absolutely lost for the process ($-\dot{Q} = 0$). This heating process is theoretically possible, but it will run at a lower thermal efficiency of the furnace chamber.
2. Using the heat surplus in other computational zones ($-\dot{Q} \neq 0$). For this heating, greater efficiency of the furnace chamber will be achieved. This heating process will, however, deviate slightly from the linearity of surface temperature increase during heating up.

For the ideal process, unit heat consumption increases with increasing heating rate (Fig.10) and is contained in the range:

- 943 to 1277 kJ/kg – for ($-\dot{Q} \neq 0$), and
- 974 to 1722 kJ/kg – for ($-\dot{Q} = 0$).

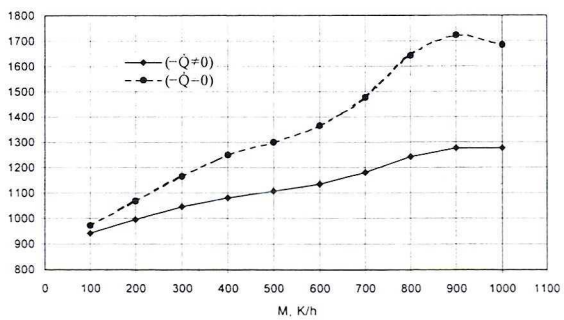

Fig. 10. Effect of heating rate on heat consumption of the ideal process

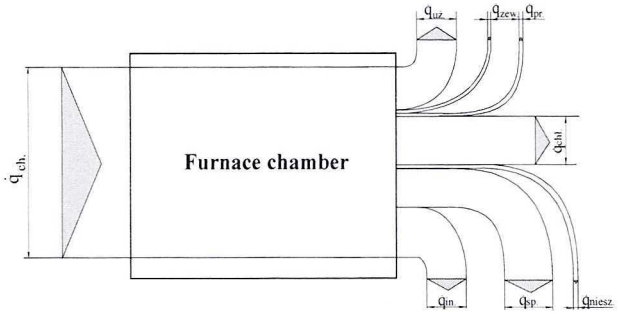

Fig.11. Sankey's heat balance diagram for a furnace attaining high indices

For a furnace attaining high indices, the balance on the output side (Fig. 11) is composed of the following items:

1. Charge usable heat.
2. Losses of heat through the walls. These losses were calculated assuming the value of coefficient of heat transfer through the walls equal to $k = 0.8\ \mathrm{W/(m^2 \cdot K)}$.
3. Heat of radiation through the furnace openings. These losses were calculated by assuming the surface area of furnace openings.
4. Cooling water heat. These losses were calculated by assuming the surface areas of slide rails in particular furnace zones.
5. Heat losses through leaks. The magnitudes of these losses were calculated for each computational zone by using the relationship below:

$$\dot{Q} = 100\left(\frac{t_{sp}}{1000}\right)^{1.3}. \tag{38}$$

6. Combustion-gas heat losses. These losses were calculated for the temperature of combustion gas leaving the furnace.
7. Other losses. A time-constant value of these losses of 8.0 MW was assumed.

The computation results (Fig.12) indicate that there is a specific heating rate for this tcase of heating, which ensures the minimum heat consumption. This is fully consistent with the results of theoretical analysis.

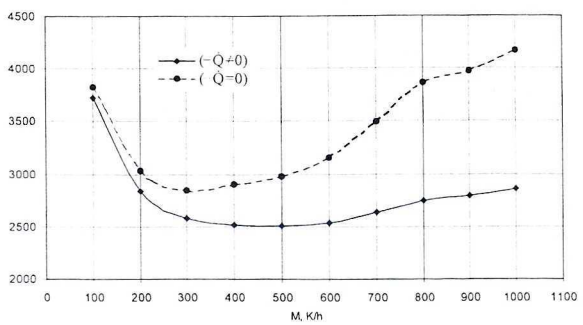

Fig.12. Effect of heating rate on heat consumption for a furnace attaining high indices

For the furnace attaining low indices, the item "other losses" was omitted on the output side of the balance, and the items "cooling water heat" and „heat losses through leaks" were reduced.

The computation results (Fig.13) show that for this case of heating, the minimum heat consumption is obtained for small heating rates. Further increase in heating rate results in an increase in heat consumption. This process is close to the ideal process.

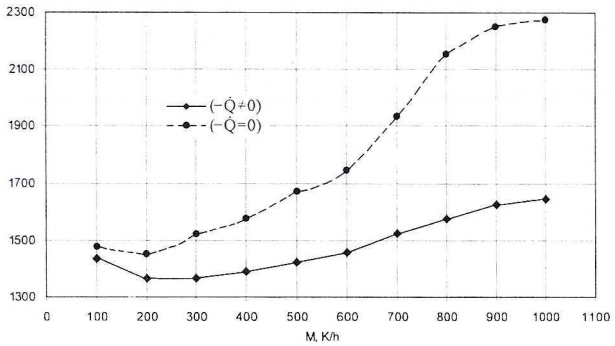

Fig. 13. Effect of heating rate on heat consumption for a furnace attaining low indices

6. Model studies on the technology of energy-saving heating of steel charge

Three cases of charge surface temperature variation during heating, described by the general equation (37) were subjected to the analysis of the effect of heating rate on heat consumption.

The following values of the exponent G were considered in the analysis: $G = 1.0$; $G = 0.8$; $G = 0.6$.

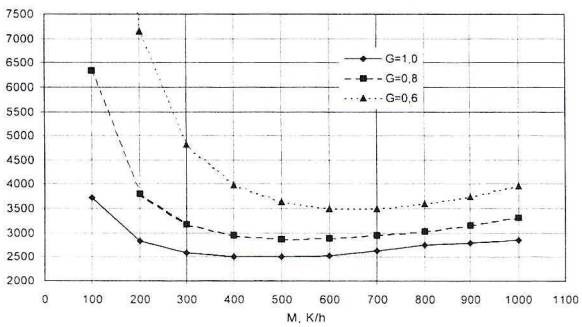

Fig. 14. Effect of heating rate on heat consumption for a furnace attaining high indices

The computations results (Fig.14) show that for each heating case a specific heating rate exists, which ensures the minimum heat consumption. This is in full agreement with

the results of theoretical analysis. At the same time, this confirms the thesis that the most energy-saving technology is heating with a linear increase of charge surface temperature. The more surface temperature variation deviates from linearity, the higher heat consumption indices are obtained.

The computation results indicate that heating technology has crucial effect on the values of heat consumption indices. Changing heating technology from G1 to G3 causes an increase in heat consumption for particular heating rates by from 30 to almost 350%.

At the same time, great saving effects are brought about by conducting heating with the appropriate values of heating rates. Changing from the heating rate 100K/h to the rational values (500–600K/h) causes a reduction of heat consumption by over 30% for G_1 and by almost 80% for G_3.

7. Conclusions

From the results of analyses and computations carried out, the following conclusions can be drawn:

1. The results of numerical modeling show that for each case of heating a specific heating rate exists, which assures the minimum heat consumption.
2. The results of a computer simulation of the effect of heating rate on heat consumption clearly indicate that the most energy-saving process is heating with a "nearly" linear variation of charge surface temperature.
3. The results of modeling by two methods used are similar.
4. Significant differences in the values of determined temperatures occur only in the first two computational furnace zones (10% of the furnace length).
5. For heating with a linear increase of surface temperature, relative differences in temperatures for the first balance zone are 15%, whereas about 5% for the second zone. For the end zones, relative differences in the values of computed temperatures are less than 0.1%.
6. For heating processes close to real processes, relative differences in the values of temperatures for the first zone are less than 3%.

REFERENCES

[1] Z. Kolenda, Transport ciepła i masy w procesach metalurgicznych. Cz.I. Przewodzenie ciepła. Problemy liniowe. AGH Kraków (1982).
[2] E. Kostowski, Przepływ ciepła. Wyd.II. Pol. Śląska, Gliwice (1991).
[3] Zb. Wernicki, I. Krężołek, Dynamika procesów cieplnych. Polit. Częst., Częstochowa (1976).
[4] E. Kostowski, Zeszyty Naukowe Pol. Śląskiej. Energetyka **49**, Gliwice (1973).
[5] M. Kieloch, Archives of Metallurgy **4**, 371 (1991).
[6] M. Kieloch, Technologia i zasady obliczeń nagrzewania wsadu. Wydawnictwo Pol. Częstochowskiej, Częstochowa (1995).

[7] M. Kieloch, T. Wyleciał, Mat. Ogólnopolskiej Konf. Gospodarka cieplna i eksploatacja pieców przemysłowych. Częstochowa-Poraj (1993).
[8] B. Mochnacki, J.S. Suchy, Modelowanie i symulacja krzepnięcia odlewów. Wydawnictwo Naukowe PWN, Warszawa (1993).
[9] J. Szargut i in., Mat. Sem. Przepływ ciepła w procesach nagrzewania i chłodzenia metali. Ustroń – Jaszowiec (1986).
[10] J. Szargut i in., Modelowanie numeryczne pól temperatury, Wydawnictwo Naukowo-Techniczne, Warszawa (1992).
[11] W. Luty, i in., Poradnik Inżyniera – Obróbka cieplna stopów żelaza, Wydawnictwo Naukowo-Techniczne, Warszawa (1977).
[12] Z. Rudnicki, Radiacyjny przepływ ciepła w piecach przemysłowych. Wyd. Pol. Śląskiej. Wyd. 2, Gliwice (1992).

REVIEWED BY: ZYGMUNT KOLENDA

Received: 7 October 2001.